科技部補助專題研究計畫成果報告
期末報告

密度泛函數理論對兩個化學系統的適用性以及精確性

計 畫 類 別 ：個別型計畫
計 畫 編 號 ：MOST 102-2113-M-040-005-
執 行 期 間 ：102 年 08 月 01 日至 104 年 07 月 31 日
執 行 單 位 ：中山醫學大學醫學應用化學系(含碩士班)

計 畫 主 持 人 ：賴金宏

計畫參與人員：學士級-專任助理人員：黃品淇

處 理 方 式 ：
1.公開資訊：本計畫可公開查詢
2.「本研究」是否已有嚴重損及公共利益之發現：否
3.「本報告」是否建議提供政府單位施政參考：否

中 華 民 國 104 年 07 月 24 日

中 文 摘 要 ： 在這項研究中，以幾個密度泛函理論（DFT）和 CBS-QB3 計算方法對環狀烷基胺基碳烯基與亞硼基所形成之錯合物其性質進行探討，我們還考慮了許多不同的構相(conformer)。2011 年，kinjo 等人成功地使用兩個飽和的環狀烷基胺基碳烯基合成了一個具有路易斯鹼性的硼衍生物。在這項工作中，我們比較了不飽和環狀烷基胺基碳烯基與飽和的環狀烷基胺基碳烯基對此硼衍生物性質的影響。根據我們的研究結果，不飽和環狀烷基胺基碳烯基會降低此種硼衍生物的質子親合力。根據自然鍵結軌域分析的結果，此種硼衍生物的中心硼原子上具有的孤對電子對是在一個 pi 型 p 軌道上。

中文關鍵詞： 硼，密度泛函數理論，環狀烷基胺基碳烯基，自然鍵結軌域分析

英 文 摘 要 ： In this study, several density functional theory (DFT) and CBS-QB3 calculations were performed to explore the properties of different conformers of cyclic (alkyl) (amino) carbene (CAAC) borane complexes with the chemical formula BH(C4NH5)2. In 2011, Kinjo et al. successfully synthesized a Lewis-basic boron derivative using two saturated CAACs (Kinjo et al., 2009). In this work, the properties of the boron atom attached to two unsaturated CAACs and two saturated CAACs were compared. According to our results,
the unsaturated CAAC shows reduced proton affinity of the boron atom as compared to the saturated CAAC；
the insertion of two C@C double bonds into CAAC makes the BACcarbenic bonds stronger. The results of natural bond orbital analysis indicated that the lone pair of the central boron atom can be viewed as a pure p-type p orbital.

英文關鍵詞： Boron, DFT, Cyclic (alkyl) (amino) carbene, Natural bond orbital analysis

Computational and Theoretical Chemistry 1051 (2015) 17–23

Contents lists available at ScienceDirect

Computational and Theoretical Chemistry

journal homepage: www.elsevier.com/locate/comptc

Computational study of unsaturated and saturated cyclic (alkyl) (amino) carbene borane complexes

Pin-Qi Huang, Chin-Hung Lai *

School of Applied Chemistry, Chung Shan Medical University, 402 Taichung, Taiwan
Department of Medical Education, Chung Shan Medical University Hospital, 402 Taichung, Taiwan

ARTICLE INFO

Article history:
Received 5 July 2014
Received in revised form 6 September 2014
Accepted 26 October 2014
Available online 1 November 2014

Keywords:
Boron
DFT
CBS-QB3
Cyclic (alkyl) (amino) carbene
Natural bond orbital analysis

ABSTRACT

In this study, several density functional theory (DFT) and CBS-QB3 calculations were performed to explore the properties of different conformers of cyclic (alkyl) (amino) carbene (CAAC) borane complexes with the chemical formula $BH(C_4NH_5)_2$. In 2011, Kinjo et al. successfully synthesized a Lewis-basic boron derivative using two saturated CAACs (Kinjo et al., 2009). In this work, the properties of the boron atom attached to two unsaturated CAACs and two saturated CAACs were compared. According to our results, the unsaturated CAAC shows reduced proton affinity of the boron atom as compared to the saturated CAAC; the insertion of two C=C double bonds into CAAC makes the B—$C_{carbenic}$ bonds stronger. The results of natural bond orbital analysis indicated that the lone pair of the central boron atom can be viewed as a pure π-type p orbital.

1. Introduction

Although boron is positioned adjacent to carbon in the periodic table, it does not share the same degree of versatility as the latter in chemical reactions. In contrast to the partially filled p orbitals of carbon, boron has an empty p orbital that typically renders boron-containing compounds Lewis acidic. Interestingly, it was shown that a monovalent-boron center bearing an electron pair, such as a borylene (Scheme 1), may have its valence electrons available and act as a Lewis base instead [1–18]. For example, Timms found that BF is reactive toward alkynes [1,2]. However, borylenes have generally been considered as transient intermediates. For instance, in their study on the metal reduction of arylboron dihalides, Grigsby and Power determined that a borylene can undergo intramolecular insertions into C—C σ bonds [3]. Moreover, according to Ito et al., photoreaction of $TbtB(SeMe)_2$ with benzyl and phenanthrenequinone involves the borylene TbtB (Tbt: 2,4,6-tris[bis-(trimethylsilyl)methyl]phenyl) as a transient intermediate [4]. Recently, a NHC-stabilized borylene was identified as an intermediate in the photochemical isomerization of C,C-chelate $BMes_2$ [5]. In order to stabilize borylenes, transition metals are typically used in synthesis. Indeed, the chemistry of transition metal-borylene complexes is well developed and a number of reviews have been published [6–11]. Similarly, nucleophilic carbenes, which can act simultaneously as σ-donors and π-acceptors, have also been employed to stabilize borylenes [12–16]. In particular, Kinjo et al. synthesized neutral and basic boron derivatives employing two cyclic (alkyl) (amino) carbenes (CAACs) to stabilize the parent borylene (:B—H, see **1** in Scheme 1) [15,16]. Because of its sp-hybridization, the parent borylene (with R=H, Scheme 1) is linear.

As the borylene accepts the two carbenic lone pairs in **1**, the lone pair of the central boron atom changes from a sp hybridized orbital to a p orbital [15]. Two resonance structures are thus possible for **1**, e.g., **1a** and **1b** (Scheme 1). In the former, a lone pair sits on the central boron atom; in the latter, two valence electrons of the boron atom are associated with the formation of a B=C double bond. Remarkably, the existence of these resonance structures has been confirmed by structural studies [15]. In **1**, the boron atom is believed to adopt a trigonal planar geometry with a bond length of ~1.52 Å with the carbenic carbon, which is in between the distance of the B—C single-bond in carbene-BH_3 complexes (1.585 ± 0.004 Å) and that of the B=C double-bond (1.31–1.42 Å) of methyleneborane derivatives [15,19,20]. In addition, the basicity of **1** has been demonstrated experimentally through protonation by trifluoromethanesulfonic acid to form **[1H]**$^+[CF_3SO_3]^-$ [15]. Moreover, the proton affinity of **1** was estimated to be 1108.0 kJ/mol from BP86/def2-SVP gas-phase calculations using zero-point energy correction [15].

Although no experimental data about the CAAC with an unsaturated C=C bond are available, its analog, N-heterocyclic carbene (NHC), exists in both saturated and unsaturated forms [21,22]. In

* Corresponding author at: School of Applied Chemistry, Chung Shan Medical University, 402 Taichung, Taiwan.
E-mail address: chlai125@csmu.edu.tw (C.-H. Lai).

http://dx.doi.org/10.1016/j.comptc.2014.10.029
2210-271X/

2009, Chang and coworkers reported that the saturated NHC—Ir complex [(sat-NHC—Bn)Ir(CO)(PR_3)]Cl appears to be slightly more active than the unsaturated NHC—Ir complex [(un-NHC—Bn)Ir(CO)(PR_3)]Cl in catalyzing the amine N-alkylation with alcohol, via a hydrogen-transfer reduction [23]. Although both the sat-NHC—Bn and the un-NHC—Bn are characterized by the same Ir—$C_{carbenic}$ bond length, they exert a different influence on the electronic properties of the complex, resulting in different catalysis efficiency. Therefore, the effect of inserting an unsaturated C=C double bond into the CAAC on the basicity of the central boron atom was explored in this study. In order to do so, sixteen different density functional theory (DFT) methods and CBS-QB3 were employed to explore the electronic structures of the conformers of $BH(C_4NH_5)_2$. Furthermore, a comparison between $BH(C_4NH_5)_2$ and its saturated analog $BH(C_4NH_7)_2$ was carried out. DFT is a quantum mechanical modeling method used to investigate the electronic structure of many-body systems such as atoms and molecules. According to this theory, the properties of a many-electron system can be determined using functionals, i.e., the functions of spatially dependent electron density. The relatively low computational costs of DFT compared to that of the post-SCF methods have made it the most popular method available in condensed-matter physics, computational physics, and computational chemistry [24–28]. However, the accuracy of DFT may be greatly improved by choosing appropriate exchange and correlation interactions. Despite recent improvements, no systematic approach has been proposed to improve DFT methods with the aim of achieving a chosen level of accuracy. Therefore, sixteen DFT methods are selected and compared with the CBS-QB3 results in this study.

In particular, the CBS-QB3 data obtained for one of the conformers (**2** in Scheme 2) of the prototypical molecule $BH(C_4NH_5)_2$ indicate that **2** is not a minimum of the potential energy surface [29], but represents a transition state with one imaginary frequency. Visual inspection of the motion corresponding to the imaginary frequency (Fig. 1) of **2** suggests that $BH(C_4NH_5)_2$ possesses a minimum on its potential energy surface designated as **3** or **4** (Scheme 2). Indeed, the CBS-QB3 results indicate that both **3** and **4** are minima of the potential energy surface of $BH(C4NH_5)_2$, the relative energy (with respect to **2**) of **3** and **4** being −20.6 and −30.7 kJ/mol, respectively.

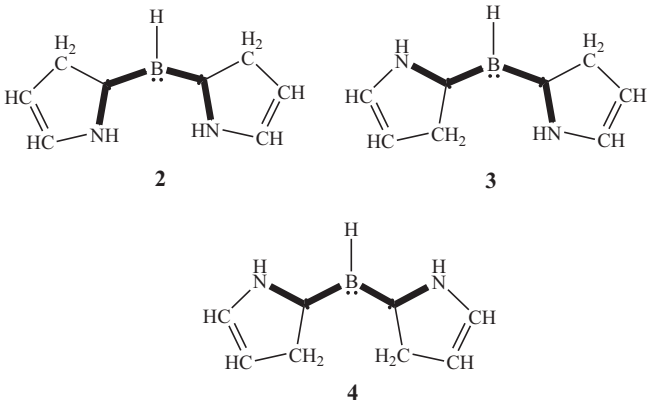

Scheme 2. Proposed conformers of the prototypical molecule $BH(C_4NH_5)_2$.

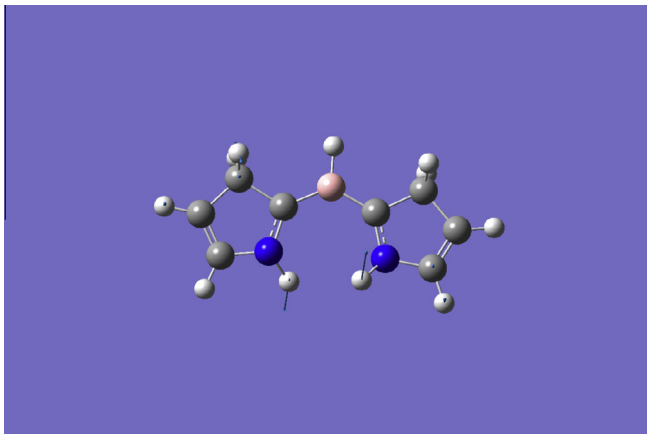

Fig. 1. Motion corresponding to the imaginary frequency of **2** calculated with the CBS-QB3 method.

2. Computational details

All calculations performed in this work were carried out with the Gaussian09 software [30]. The CBS-QB3 extrapolation-based

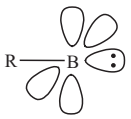

borylene

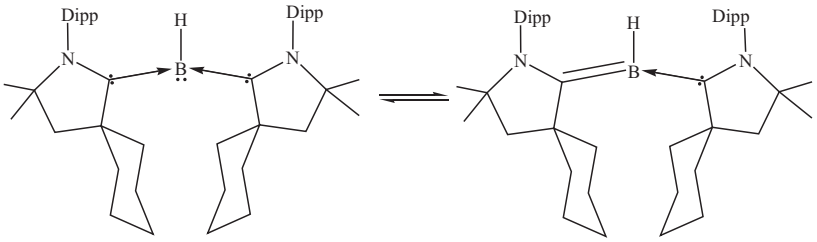

Dipp = 2,6-diisopropylphenyl

1a **1b**

Scheme 1. Structure of a borylene.

composite method, applied on geometries optimized with the B3LYP functional, shows a mean absolute error of 3.6 kJ/mol for the G2 test set [29]; it was thus employed as a reference for the investigation of the accuracy of the various DFT methods used in this work.

The DFT methods selected for this study can be categorized as follows: (1) six hybrid GGA functionals (B3LYP, B3P86, B3PW91, MPW1LYP, MPW1PW91, MPW1K); (2) six hybrid meta-GGA functionals (M05, M06, M06-2X, PBE1KCIS, TPSSh, TPSS1KCIS); (3) two long-range corrected functionals (wB97X, and wB97XD); (4) two double-hybrid functionals (B2PLYP, and B2PLYPD) [31–47].

The double-ξ basis set D95V+** was combined with the selected DFT methods [48] for geometry optimizations and subsequent frequency calculations. All stationary points were identified as equilibrium structures according to the number of imaginary frequencies (NIMAG = 0) or transition states (NIMAG = 1). For the transition states, motions corresponding to the imaginary frequencies were visually checked. Zero-point energy (ZPE) corrections were included. Natural bond orbital (NBO) analysis was performed using NBO5.9 as implemented in Gaussian09 [49].

3. Results and discussion

3.1. Structures of 2, 3, and 4

Selected geometrical parameters of **2**–**4** (Scheme 2) are listed in Tables S1–S3. Without the resonance structure like that of **1b** (Scheme 1), the two B—$C_{carbenic}$ bonds of **2**, **3**, and **4** should have a donor–acceptor character. Therefore, the accuracy of the optimized B—$C_{carbenic}$ bond lengths obtained by the selected DFT functional in this study was compared to that obtained with a more sophisticated method, MP4(DQ)/D95V+**. Our results showed that the DFT-optimized B—$C_{carbenic}$ bond lengths are similar to the MP4-optimized ones. The B—$C_{carbenic}$ bond lengths calculated in the present study fall between the B—C single bond length in carbene-BH_3 complexes (1.59 Å) and the B=C double bond length in methyleneborane derivatives (1.44 Å) [50]. This may be an indication that similar resonance structures, such as that of **1b** (Scheme 1), may play an important role for the final geometry of $BH(C_4NH_5)_2$. The similarity of the DFT-optimized B—$C_{carbenic}$ bond lengths and the MP4-optimzied ones may indicate that both methods give a similar importance to the resonance structure like that of **1b** (Scheme 1) for **2**, **3**, and **4**. Furthermore, a comparison between our calculated B—$C_{carbenic}$ bond lengths and the values obtained from X-ray diffraction on **1** (1.5165 ± 0.0015 Å) revealed that the B—$C_{carbenic}$ bond length in $BH(C_4NH_5)_2$ is shorter than that observed in **1** [15]. All DFT methods showed that the sum of the three angles around the central boron atom equals 360° in **2**, **3**, and **4**. This result is in agreement with X-ray crystallographic studies on **1**, suggesting that the insertion of a double bond into CAACs hardly affect the hybridization of the central boron atom, which is sp^2 in all complexes.

The analysis of the vibrational frequencies of **2** showed that the final structures of $BH(C_4NH_5)_2$ obtained from all the selected DFT methods are a minimum of the potential energy surface. This result is, however, in contrast to what was found using the CBS-QB3 method. This may be due to the fact that when CBS-QB3 was used, both the ∠N—$C_{carbenic}$—B—H angles were found to be 180°, unlike those calculated with DFT.

The calculated dipole moments (debye), rotational constants (GHz), and vibrational frequencies (cm^{-1}) of **2** are listed in Table S4. According to the calculated dipole moment, **2** was identified as a polar molecule. The asymmetric parameter (κ) can be obtained from the calculated rotational constants (Eq. (1)). When κ = 1, the molecule is an oblate symmetric top; when κ = −1, the molecule is a prolate symmetric top.

$$\kappa = \frac{(2B - A - C)}{(A - C)} \tag{1}$$

According to all DFT calculations performed in this study, the asymmetric parameter was estimated to be close to −1, which indicates that **2** is a prolate symmetric top (Table S4).

3.2. Accuracy of selected DFT functionals

In order to explore the accuracy of the DFT methods, DFT results were compared with those obtained using CBS-QB3. Conformer **2** was arbitrarily taken as the zero-energy point; the DFT-calculated relative energies of **3** and **4** ($E_{3\to2}$, and $E_{4\to2}$ in kJ/mol) are listed in Table 1 as well as those computed with the CBS-QB3 method. All methods employed in this work provided negative values for $E_{3\to2}$ and $E_{4\to2}$, indicating that both **3** and **4** are more stable than **2**, with a stability trend of **4** > **3** > **2**. To enable a quantitative comparison, the relative deviations RD1 and RD2 were introduced as follows:

$$\mathrm{RD1} = \frac{|E_{3\to2}(\mathrm{DFT}) - E_{3\to2}(\mathrm{CBS\text{-}QB3})|}{|E_{3\to2}(\mathrm{CBS\text{-}QB3})|} \times 100\% \tag{2}$$

$$\mathrm{RD2} = \frac{|E_{4\to2}(\mathrm{DFT}) - E_{4\to2}(\mathrm{CBS-QB3})|}{|E_{4\to2}(\mathrm{CBS-QB3})|} \times 100\% \tag{3}$$

where $E_{3\to2}$(DFT), $E_{4\to2}$(DFT), $E_{3\to2}$(CBS-QB3), and $E_{4\to2}$(CBS-QB3) are the relative energies to conformer **2** of **3**, and **4**, calculated with the DFT and CBS-QB3 method (Table 1).

In addition, the average relative deviation (ARD) was calculated as:

$$\mathrm{ARD} = \frac{\mathrm{RD1} + \mathrm{RD2}}{2} \tag{4}$$

Data collected in Table 1 show that the addition of empirical dispersion reduced the ARD of DFT, indicating a better performance. For instance, inclusion of dispersion in B2PLYP caused a reduction of ARD from 21.04% (B2PLYP) to 17.05% (B2PLYPD). Similarly, ARDs for wB97X and wB97XD are 24.73% and 18.49%, respectively. Data in Table 1 also show that the best performing DFT method is PBE1KCIS, the ARD being the smallest,

Table 1
$E_{3\to2}$, $E_{4\to2}$ (kJ/mol), RD1, RD2, and ARD of several DFT functionals.

	$E_{3\to2}$[a]	$E_{4\to2}$[b]	RD1[c] (%)	RD2[d] (%)	ARD[e] (%)
B3LYP	−16.2	−25.8	21.27	15.70	18.49
B3P86	−16.9	−27.2	18.07	11.43	14.75
B3PW91	−16.6	−26.4	19.46	13.74	16.60
MPW1LYP	−16.2	−25.9	21.37	15.45	18.41
MPW1PW91	−16.7	−26.8	18.81	12.72	15.76
MPW1K	−16.4	−26.6	20.17	13.24	16.70
M05	−15.5	−25.5	24.61	16.97	20.79
M06	−17.0	−27.3	17.27	11.08	14.18
M06-2X	−15.7	−26.0	23.74	15.06	19.40
PBE1KCIS	−17.1	−27.5	16.96	10.33	13.64
TPSSh	−16.7	−26.6	18.74	13.19	15.96
TPSS1KCIS	−16.6	−26.6	19.15	13.34	16.25
B2PLYP	−15.6	−25.2	24.18	17.91	21.04
B2PLYPD	−16.2	−26.7	21.18	12.92	17.05
wB97X	−14.9	−24.0	27.74	21.72	24.73
wB97XD	−16.5	−25.5	20.03	16.96	18.49
CBS-QB3	−20.6	−30.7	–	–	–

[a] $E_{3\to2} = E(\mathbf{3}) - E(\mathbf{2})$.
[b] $E_{4\to2} = E(\mathbf{4}) - E(\mathbf{2})$.
[c] See Eq. (2).
[d] See Eq. (3).
[e] See Eq. (4).

13.64%. This finding demonstrates that the PBE1KCIS/D95V+** level of theory can be used to provide an accurate theoretical description of the electronic properties of $BH(CAAC)_2$. The following discussion is therefore based only on data obtained at this level of theory.

3.3. Comparison of the calculated results obtained for 2–4

As shown by the PBE1KCIS-optimized dipole moment (debye), rotational constants (GHz), and zero-point energy (hartree) in Table 2, **2–4** can all be considered polar molecules, as their dipole moments are not zero. Moreover, **2**, **3**, and **4** were all shown to be prolate symmetric tops, as their asymmetric parameters are close to −1.

Because different conformers may have a different reactivity [51,52], we explored the possibility for the conformers **2**, **3**, and **4** to have different activities toward proton using PBE1KCIS/D95V+**. The optimized geometries of the protonated complexes (**2H**$^+$, **3H**$^+$, and **4H**$^+$) are shown in Fig. S1, and structural data collected in Table 3. Our data showed that the B—$C_{carbenic}$ and B—H bond lengths increase when the studied conformers are protonated, while the bond angle, ∠$C_{carbenic}$—B—$C_{carbenic}$, decreases. As shown in Tables 3, 2 has the largest proton affinity, the overall trend being **2** > **3** > **4**.

Further data about the electronic properties of conformers **2**, **3**, **4**, and protonated derivatives **2H**$^+$, **3H**$^+$, **4H**$^+$ were produced by performing the NBO analysis (Table 4). According to the NBO analyses of **2**, **3**, and **4**, the two B—$C_{carbenic}$ bonds have the same bond order value (larger than 1, calculated using the method developed by Wiberg) [53], and resonance structures like that of **Ib** (Scheme 1) are possible for all the studied conformers. If only structures like that of **1a** (Scheme 1) existed, the two B—$C_{carbenic}$ bonds of **2**, **3**, and **4** would have a donor–acceptor character and bond orders smaller than 1. The negative charge of the boron atom and the positive charge of the carbenic center increased upon protonation of $BH(C_4NH_5)_2$, indicating that the ionic character of the B—$C_{carbenic}$ bond is strengthened by the addition of H^+. In contrast, the covalent character of the B—$C_{carbenic}$ bond decreased, in line with the changes in the calculated bond order. A similar change in bond order was estimated for the B—H bond. According to the NBO analysis, a lone pair exists on the central boron atom of conformers **2**–**4**, which can be viewed as a pure π-type p orbital (Table 4).

3.4. Comparison between 4 and its saturated analog SAT4

Additional PBE1KCIS calculations were performed in order to compare **4**, the most stable conformer of $BH(C_4NH_5)_2$, with its saturated analog, **SAT4**. Their protonated complexes are also compared in this study. The geometries of **4**, **4H**$^+$, **SAT4**, and **SAT4H**$^+$ are displayed in Fig. 2. The optimized B—$C_{carbenic}$ bond lengths in **SAT4** are typically shorter than those of the X-ray structure of **1** [15]. This discrepancy may be attributed to two possible reasons: (i) the effect of crystal packing, which is neglected in our gas-phase calculations [54,55]; (ii) the steric hindrance caused by the cyclohexyl groups in **1**, which may play an important role in determining its final structure [15]. Moreover, saturated and unsaturated CAACs form B—$C_{carbenic}$ bonds characterized by similar bond lengths (Fig. 2); however, the $C_{carbenic}$—N bonds in **SAT4** show slightly smaller bond lengths than those in **4**. Table 5 lists the results of the NBO analysis of **4**, **4H**$^+$, **SAT4**, and **SAT4H**$^+$. Interestingly, the lone pair of the boron atom in **SAT4** can also be viewed

Table 2
Calculated dipole moments (debye), rotational constants (GHz), asymmetric parameters (hartree), and zero-point energies (hartree) of **2**, **3**, and **4**.

	2	**3**	**4**
Dipole moment	3.13	1.88	0.0921
Rotational constants	3.52	3.54	3.52
	0.560	0.553	0.555
	0.490	0.481	0.482
Asymmetric parameter (κ)	−0.954	−0.953	−0.952
Zero-point energy	0.180	0.180	0.180

Table 3
Selected geometrical parameters of **2H**$^+$–**4H**$^+$ and proton affinity of **2**–**4** (bond length in Å, bond angle in °, and proton affinity in kJ/mol).

X	R(B—$C_{cabenic}$)[a]	∠$C_{carbenic}$—B—$C_{carbenic}$[a]	R(B—H)[a]	Δ*E* of **X** + H^+ → **XH**$^+$
2	1.583 (1.494)	119.3 (122.2)	1.220 (1.205)	−1035
3	1.585 (1.493)	118.2 (122.2)	1.221 (1.209)	−1024
4	1.581 (1.491)	119.4 (120.6)	1.223 (1.212)	−1014

[a] Average values.

Table 4
Results of the NBO analysis of **2**–**4**, and **2H**$^+$–**4H**$^+$.

	q(B)[a]	*q*($C_{carbenic}$)[a]	BO(B—$C_{carbenic}$)[b]	BO(B—H)[b]	E_{LP}(B)[c]	OP_{LP}(B)[d]	Hybrids of lone pair of boron atoms
2	−0.0826	0.0718	1.288	0.9544	0.0327	0.7150	s: 0.00% p: 99.96% d: 0.03% f: 0.01%
3	−0.0792	0.0703 0.0512	1.271 1.297	0.9558	0.0328	0.7223	s: 0.00% p: 99.96% d: 0.03% f: 0.01%
4	−0.0708	0.0596	1.281	0.9567	0.0307	0.7172	s: 0.00% p: 99.93% d: 0.04% f: 0.03%
2H$^+$	−0.4292	0.3396 0.3224	0.9860 0.9819	0.8761 0.8945	–	–	–
3H$^+$	−0.4201	0.3329	0.9762	0.8939	–	–	–
4H$^+$	−0.4189	0.3319	0.9855	0.9462 0.8240	–	–	–

[a] *q*(X) represents the charge on the X atom.
[b] BO is the abbreviation of bond order.
[c] E_{LP} is the energy of the lone pair (eV).
[d] OP_{LP} is the occupancy of the lone pair.

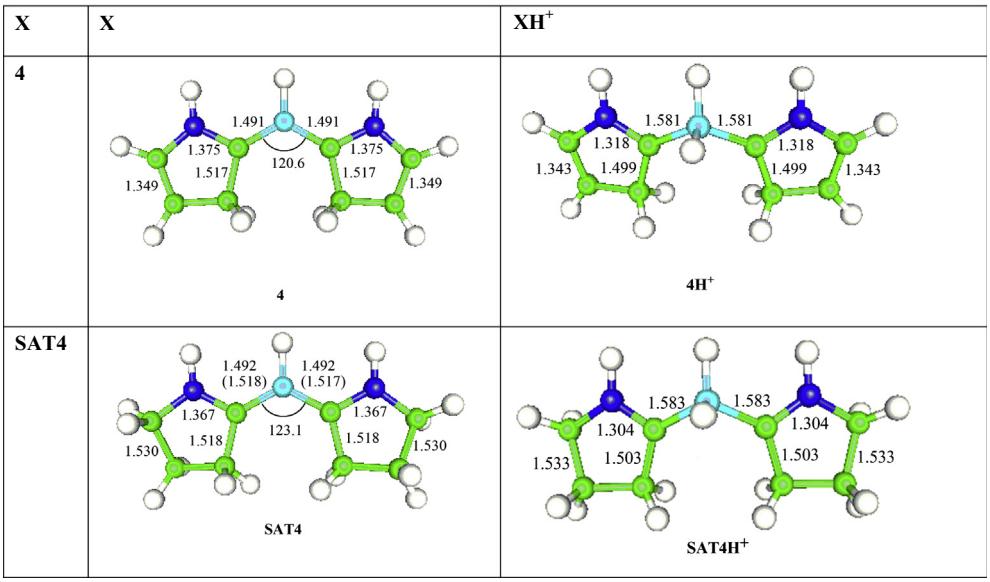

Fig. 2. PBE1KCIS-optimized geometries of **4**, **4H**$^+$, **SAT4**, and **SAT4H**$^+$ (bond length in Å, bond angle in °; boron in sky blue, carbon in green, nitrogen in blue, hydrogen in white; the values in parentheses are those of the X-ray crystallographic study on **1**). (For interpretation of the references to colour in this figure legend, the reader is referred to the web version of this article.)

Table 5
NBO analysis of **4**, **4H**$^+$, **SAT4**, and **SAT4H**$^+$.

	4	**4H**$^+$	**SAT4**	**SAT4H**$^+$
q(B)[a]	−0.0708	−0.4189	−0.1189	−0.4116
q($C_{carbenic}$)[a]	0.0596	0.3319	0.0707	0.3510
BO(B—$C_{carbenic}$)[b]	1.281	0.9855	1.295	0.9763
BO(B—H)[b]	0.9567	0.9462	0.9542	0.9537
		0.8240		0.8257
E_{LP}(B)[c]	0.0307	–	0.0412	–
OP_{LP}(B)[d]	0.7172	–	0.7752	–
Hybrids of lone pair of boron atoms	s: 0.00% p: 99.93% d: 0.04% f: 0.03%	–	s: 0.00% p: 99.92% d: 0.05% f: 0.03%	–

[a] q(X) represents the charge on the X atom.
[b] BO is the abbreviation of bond order.
[c] E_{LP} is the energy of the lone pair (eV).
[d] OP_{LP} is the occupancy of the lone pair.

as a pure π-type p orbital, as observed in **4**, however showing a greater energy than that in **4**. This finding is mirrored by the calculated proton affinity of **SAT4** (1058.9 kJ/mol), which is 44.6 kJ/mol larger than that of **4**.

Fig. 3 illustrates the frontier orbitals of **4** and **SAT4**, in which the two highest occupied molecular orbitals (HOMOs) of **4** and **SAT4** appear as a mixture of the lone pair of the central boron atom and the π∗ orbitals of the two CAACs; the two lowest unoccupied molecular orbitals (LUMOs) involve the π∗ orbitals of the two CAACs.

Inspired by a study of Rablen and coworkers, who used high-level ab initio calculations to find possible differences in the sequential B—C bond energies for borane [56], we explored this aspect for both **4** and **SAT4**. The PBE1KCIS method was thus used to calculate the sequential B—$C_{carbenic}$ bond dissociation energies (BDEs), defined as in Eq. (5), where X = C_4NH_5, or C_4NH_7, and in Eq. (6), where BH is considered in its singlet state.

$$BDE1 = E(BHX) + E(X) - E(BHX_2) \quad (5)$$

$$BDE2 = E(BH) + E(X) - E(BHX) \quad (6)$$

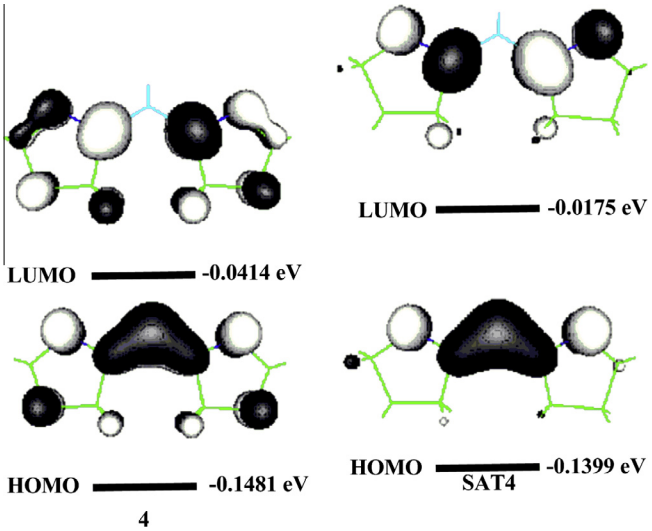

Fig. 3. Frontier orbitals of **4** and **SAT4** (isodensity value = 0.05).

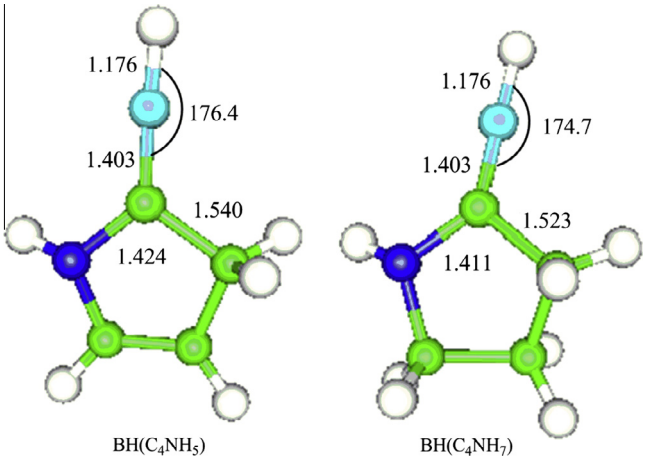

Fig. 4. PBE1KCIS-optimized geometries of $BH(C_4NH_5)$, and $BH(C_4NH_7)$ (bond length in Å, bond angle in °).

The PBE1KCIS-optimized geometries of the fragments $BH(C_4NH_5)$ and $BH(C_4NH_7)$ are depicted in Fig. 4. BDE1 and BDE2 of **4** and **SAT4** were calculated to be 401.9 and 398.9 kJ/mol, and 381.2 and 393.8 kJ/mol, respectively. The difference between BDE1 and BDE2 (ΔBDE) in **4** is negligible (3.0 kJ/mol), considering the uncertainty of the calculation method employed in this work [57]. ΔBDE becomes significant for **SAT4**, −12.6 kJ/mol. This can be easily rationalized by the fact that a partial double bond of a sp-hybridized boron with a sp^2-hybridized carbon is stronger than that of a sp^2-hybridized boron with a sp^2-hybridized carbon. A further analysis showed that **SAT4** has smaller BDE1 and BDE2 than **4**, by 20.8 kJ/mol and 5.1 kJ/mol, respectively (Table 6).

Moreover, the hybridization of the central boron atom in **4** and **SAT4** changed from sp^2 to sp, when one carbene was removed. In addition, the NBO analysis on $BH(C_4NH_5)$ and $BH(C_4NH_7)$, displayed in Table 7, provided two important information: (i) the bond order between boron and the carbenic center is 1.718 and 1.699 for $BH(C_4NH_5)$ and $BH(C_4NH_7)$, respectively; (ii) the lone pair on the central boron atom for $BH(C_4NH_5)$ and $BH(C_4NH_7)$ can also be viewed as a pure π-type p orbital.

Table 6
BDE1, BDE2 (kJ/mol) of **4** and **SAT4**.

	4	SAT4
BDE1	401.9	381.2 (−20.8)[a]
BDE2	398.9	393.8 (−5.1)[b]
ΔBDE	3.0	−12.6

[a] The value in brackets was calculated as BDE1(**SAT4**) − BDE1(**4**).
[b] The value in brackets was calculated as BDE2(**SAT4**) − BDE2(**4**).

Table 7
Results of the NBO analysis of $BH(C_4NH_5)$, $BH(C_4NH_7)$, and BH.

	$BH(C_4NH_5)$	$B(C_4NH_7)$	BH
$q(B)$[a]	0.5004	0.4553	0.3400
$q(C_{carbenic})$[a]	−0.3744	−0.3693	–
$BO(B—C_{carbenic})$[b]	1.718	1.699	–
BO(B—H)[b]	0.9902	0.9898	0.8896
$E_{LP}(B)$[c]	0.0525	0.0532	−0.3679
$OP_{LP}(B)$[d]	0.0412	0.0474	1.998
Hybrids of lone pair of boron atoms	s: 0.02% p: 99.61% d: 0.31% f: 0.06%	s: 0.09% p: 99.48% d: 0.37% f: 0.06%	s: 89.13% p: 10.85% d: 0.01% f: 0.01%

[a] $q(X)$ represents the charge on the X atom.
[b] BO is the abbreviation of bond order.
[c] E_{LP} is the energy of the lone pair (eV).
[d] OP_{LP} is the occupancy of the lone pair.

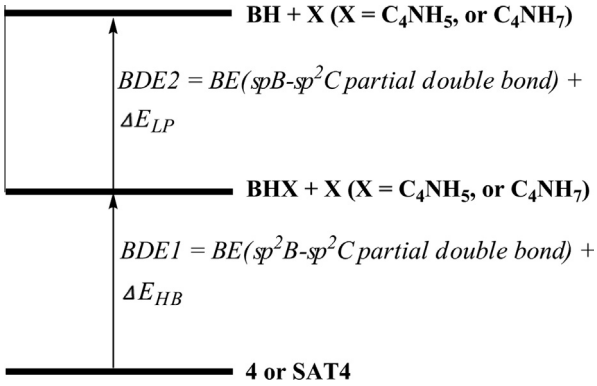

Scheme 3. Schematic representation of the sequential $B—C_{carbenic}$ bond dissociations of **4** and **SAT4.**

The sequential $B—C_{carbenic}$ bond dissociations of **4** and **SAT4** are depicted in Scheme 3, where BE represents the bond energy, ΔE_{HB} the energy involving the hybridization of the central boron atom change from sp^2 to sp, ΔE_{LP} the energy associated to the jump of the lone pair electrons of the boron atom from a π-type p orbital to a sp-hybridized orbital. We are currently investigating the factors that may influence these energetic values.

4. Conclusions

In this work, several properties of CAAC borane complexes were explored by performing calculations with several DFT methods. The comparison of these calculations with those carried out with CBS-QB3 showed that PBE1KCIS is the best performing DFT method for the studied complexes. The following conclusions can then be drawn from the calculations carried out with the PBE1KCIS method on saturated and unsaturated $BH(CAAC)_2$ complexes:

(1) Among the three conformers studied in this work (**2**, **3**, **4** in Scheme 2), **4** was found to be the most stable.
(2) Although its analog, NHC, exists in both saturated and unsaturated forms, the existence of CAAC in the unsaturated form (containing a C=C double bond) has not be proven yet. In this study, the unsaturated CAAC is predicted to reduce the proton affinity of $BH(CAAC)_2$; in addition, the $B—C_{carbenic}$ bonds are stronger.
(3) According to the results of the NBO analysis, a lone pair exists on the boron atom in $BH(CAAC)_2$, which can be viewed as a pure π-type p orbital of boron.
(4) While the sequential $B—C_{carbenic}$ bond energies of **4** are nearly the same, our calculations indicate that those of **SAT4** differ by 12.6 kJ/mol.

Kinjo et al. concluded that compounds such as **1** (Scheme 1) can act as Lewis bases, in a manner similar to those of amines and phosphines [15]. However, boron has a lower electronegativity than nitrogen and phosphorus. Therefore, it can be concluded that $BH(CAAC)_2$ is a strong electron-donating ligand for transition metals. The extensive characterization of the electronic properties of these carbene-stabilized borylenes carried out in this work provides a clear rationalization for this conclusion.

Acknowledgments

We are grateful to the National Center for High-Performance Computing (Taiwan) for providing computing time. We would also like to thank the Ministry of Science and Technology of Taiwan for their financial support. Special thanks are also due to the reviewers for their very helpful suggestions and comments.

Appendix A. Supplementary material

Supplementary data associated with this article can be found, in the online version, at http://dx.doi.org/10.1016/j.comptc.2014.10.029.

References

[1] P.L. Timms, J. Am. Chem. Soc. 90 (1968) 4585.
[2] P.L. Timms, Acc. Chem. Res. 6 (1973) 118.
[3] W.J. Grigsby, P.P. Power, J. Am. Chem. Soc. 118 (1996) 7981.
[4] M. Ito, N. Tokitoh, T. Kawashima, R. Okazaki, Tetrahedron Lett. 40 (1999) 5557.
[5] Y.-L. Rao, L.D. Chen, N.J. Mosey, S. Wang, J. Am. Chem. Soc. 134 (2012) 11026.
[6] H. Braunschweig, Angew. Chem. Int. Ed. 37 (1998) 1786.
[7] H. Braunschweig, M. Colling, J. Organomet. Chem. 614–615 (2000) 18.
[8] H. Braunschweig, M. Colling, Coord. Chem. Rev. 223 (2001) 1.
[9] H. Braunschweig, M. Colling, M. Eur, J. Inorg. Chem. 2003 (2003) 393.
[10] H. Braunschweig, Adv. Organomet. Chem. 51 (2004) 163.

[11] H. Braunschweig, C. Kollann, D. Rais, Angew. Chem. Int. Ed. 45 (2006) 5254.
[12] P. Bissinger, H. Braunschweig, K. Kraft, T. Kupfer, Angew. Chem. Int. Ed. 50 (2011) 4704.
[13] P. Bissinger, H. Braunschweig, A. Damme, R.D. Dewhurst, T. Kupfer, K. Radacki, K. Wagner, J. Am. Chem. Soc. 133 (2011) 19044.
[14] Y. Wang, G.H. Robinson, Inorg. Chem. 50 (2011) 12326.
[15] R. Kinjo, B. Donnadieu, M.A. Celik, G. Frenking, G. Bertrand, Science 333 (2011) 610.
[16] M.A. Celik, R. Sure, S. Klein, R. Kinjo, G. Bertrand, G. Frenking, Chem. Eur. J. 18 (2012) 5676.
[17] M. Krasowska, H.F. Bettinger, J. Am. Chem. Soc. 134 (2012) 17094.
[18] Y. Wang, G.H. Robinson, Science 333 (2012) 530.
[19] Y. Wang, B. Quillian, P. Wei, C.S. Wannere, Y. Xie, R.B. King, H.F. III Schaefer, P.v.R. Schleyer, G.H. Robinson, J. Am. Chem. Soc. 129 (2007) 12412.
[20] R.C. Fischer, P.P. Power, Chem. Rev. 110 (2010) 3877.
[21] A.J. III Arduengo, R.L. Harlow, M. Kline, J. Am. Chem. Soc. 113 (1991) 361.
[22] A.J. Arduengo III, J.R. Goerlich, W.J. Marshall, J. Am. Chem. Soc. 117 (1995) 11027.
[23] Y.H. Chang, C.F. Fu, Y.H. Liu, S.M. Peng, J.T. Chen, S.T. Liu, Dalton Trans. 2009 (2009) 861.
[24] C.J. Barden, J.C. Rienstra-Kiracofe, H.F. Schaefer III, J. Chem. Phys. 113 (2000) 690.
[25] S.T. Brown, J.C. Rienstra-Kiracofe, H.F. Schaefer III, J. Phys. Chem. A 103 (1999) 4065.
[26] B.S. Jursic, Chem. Phys. Lett. 256 (1996) 603.
[27] J. Gu, J. Wang, J. Leszczynski, Y. Xie, H.F. Schaefer III, Chem. Phys. Lett. 459 (2008) 164.
[28] M.N. Glukhovtsev, R.D. Bach, A. Pross, L. Radom, Chem. Phys. Lett. 260 (1996) 558.
[29] J.A. Montgomery Jr., M.J. Frisch, J.W. Ochterski, G.A. Petersson, J. Chem. Phys. 110 (1999) 2822.
[30] M.J. Frisch et al., GAUSSIAN 09, Revision A. 02, GAUSSIAN Inc., Wallingford, CT, 2009.
[31] A.D. Becke, Phys. Rev. A 38 (1988) 3098.
[32] C. Lee, W. Yang, R.G. Parr, Phys. Rev. B 37 (1988) 785.
[33] J.P. Perdew, J.A. Chevary, S.H. Vosko, K.A. Jackson, M.R. Pederson, D.J. Singh, C. Fiolhais, Phys. Rev. B 46 (1992) 6671.
[34] A.D. Becke, J. Chem. Phys. 98 (1993) 5648.
[35] C. Adamo, V. Barone, J. Chem. Phys. 108 (1998) 664.
[36] B.J. Lynch, P.L. Fast, M. Harris, D.G. Truhlar, J. Phys. Chem. A 104 (2000) 4811.
[37] B.J. Lynch, Y. Zhao, D.G. Truhlar, J. Phys. Chem. A 107 (2003) 1384.
[38] Y. Zhao, N.E. Schultz, D.G. Truhlar, J. Chem. Theory Comput. 2 (2006) 364.
[39] Y. Zhao, D.G. Truhlar, Theor. Chem. Acc. 120 (2008) 215.
[40] Y. Zhao, D.G. Truhlar, Acc. Chem. Res. 41 (2008) 157.
[41] Y. Zhao, D.G. Truhlar, J. Chem. Theory Comput. 1 (2005) 415.
[42] V.N. Staroverov, G.E. Scuseria, J. Tao, J.P. Perdew, J. Chem. Phys. 119 (2003) 12129.
[43] Y. Zhao, D.G. Truhlar, Phys. Chem. Chem. Phys. 7 (2005) 2701.
[44] J.-D. Chai, M. Head-Gordon, J. Chem. Phys. 128 (2008) 084106.
[45] J.-D. Chai, M. Head-Gordon, Phys. Chem. Chem. Phys. 10 (2008) 6615.
[46] S. Grimme, J. Chem. Phys. 124 (2005) 034108.
[47] T. Schwabe, S. Grimme, Phys. Chem. Chem. Phys. 9 (2007) 3397.
[48] T.H. Dunning Jr., P.J. Hay, in: H.F. Schaefer III (Ed.), Modern theoretical Chemistry, Plenum, New York, 1976.
[49] J.P. Foster, F. Weinhold, J. Am. Chem. Soc. 102 (1980) 7211.
[50] M.M. Olmstead, P.P. Power, K.J. Weese, R.J. Doedens, J. Am. Chem. Soc. 109 (1987) 2541.
[51] H. Satoha, S. Manabe, Chem. Soc. Rev. 42 (2013) 4297.
[52] Y.-P. Chang, K. Długołęcki, J. Küpper, D. Rösch, D. Wild, S. Willitsch, Science 342 (2013) 98.
[53] K.B. Wiberg, Tetrahedron 24 (1968) 1083.
[54] S. Reichman, F. Schreiner, J. Chem. Phys. 51 (1969) 2355.
[55] M.-S. Liao, Q.-E. Zhang, J. Phys. Chem. A 102 (1998) 10647.
[56] P.R. Rablen, J.F. Hartwig, J. Am. Chem. Soc. 118 (1996) 4648.
[57] W. Zheng, W. Xu, Y. Wang, Z. Chen, Comput. Theor. Chem. 1027 (2014) 116.

Gmail by Google

Chin-Hung Lai <chinhunglai@gmail.com>

Your article's usage report

1 封郵件

Elsevier Journals <journals@mail.elsevier.com> 2015年6月3日 上午5:23
回覆: Elsevier Journals <stjnlsemarketing@elsevier.com>
收件者: chlai125@csmu.edu.tw

ELSEVIER

Article Usage Alert

Your article *Computational Study of Unsaturated and Saturated Cyclic (Alkyl) (Amino) Carbene Borane Complexes*

Dear Prof. Lai,

We are pleased to present to you as a corresponding author, an overview of the performance of your article in *Computational and Theoretical Chemistry*. With Article Usage Alerts, a free service, you are able to measure the impact of your article via its usage on ScienceDirect.

Your article has been downloaded or viewed 226 times since publication.

For more details, please check here for your Article Usage Dashboard:

View Dashboard

For best results use Google Chrome or Firefox.

This information is generated especially for you, however if you would like to share your results and/or article with peers, feel free to send it through via email or the social media buttons in the Dashboard. If you have any questions about this service, please consult our Support site.

You receive this email as a service, however if you would like to stop receiving alerts, please use the unsubscribe option below.

You will receive quarterly Article Usage Alerts in the first year after publication of your article. If you would like to check your article more often, the information on the dashboard will be updated monthly. We suggest you bookmark the page and refer back to it.

Thank you for your interest.

Best wishes,

Elsevier

科技部補助計畫衍生研發成果推廣資料表

日期:2015/07/24

科技部補助計畫	計畫名稱: 密度泛函數理論對兩個化學系統的適用性以及精確性
	計畫主持人: 賴金宏
	計畫編號: 102-2113-M-040-005- 學門領域: 物理化學

無研發成果推廣資料

102 年度專題研究計畫研究成果彙整表

計畫主持人：賴金宏	計畫編號：102-2113-M-040-005-
計畫名稱：密度泛函數理論對兩個化學系統的適用性以及精確性	

成果項目			量化			單位	備註（質化說明：如數個計畫共同成果、成果列為該期刊之封面故事...等）
			實際已達成數（被接受或已發表）	預期總達成數(含實際已達成數)	本計畫實際貢獻百分比		
國內	論文著作	期刊論文	0	0	100%	篇	
		研究報告/技術報告	0	0	100%		
		研討會論文	0	0	100%		
		專書	0	0	100%		
	專利	申請中件數	0	0	100%	件	
		已獲得件數	0	0	100%		
	技術移轉	件數	0	0	100%	件	
		權利金	0	0	100%	千元	
	參與計畫人力（本國籍）	碩士生	0	0	100%	人次	
		博士生	0	0	100%		
		博士後研究員	0	0	100%		
		專任助理	0	0	100%		
國外	論文著作	期刊論文	1	1	100%	篇	
		研究報告/技術報告	0	0	100%		
		研討會論文	0	0	100%		
		專書	0	0	100%	章/本	
	專利	申請中件數	0	0	100%	件	
		已獲得件數	0	0	100%		
	技術移轉	件數	0	0	100%	件	
		權利金	0	0	100%	千元	
	參與計畫人力（外國籍）	碩士生	0	0	100%	人次	
		博士生	0	0	100%		
		博士後研究員	0	0	100%		
		專任助理	1	1	100%		

其他成果 (無法以量化表達之成果如辦理學術活動、獲得獎項、重要國際合作、研究成果國際影響力及其他協助產業技術發展之具體效益事項等，請以文字敘述填列。)	此篇論文在 2014 年 10 月被接受(Journal: Computational and Theoretical Chemistry)，2014 年 11 月放在網上，截至 2015 年 6 月 3 日，已經被下載或看過 226 次。

	成果項目	量化	名稱或內容性質簡述
科教處計畫加填項目	測驗工具(含質性與量性)	0	
	課程/模組	0	
	電腦及網路系統或工具	0	
	教材	0	
	舉辦之活動/競賽	0	
	研討會/工作坊	0	
	電子報、網站	0	
	計畫成果推廣之參與（閱聽）人數	0	

科技部補助專題研究計畫成果報告自評表

請就研究內容與原計畫相符程度、達成預期目標情況、研究成果之學術或應用價值（簡要敘述成果所代表之意義、價值、影響或進一步發展之可能性）、是否適合在學術期刊發表或申請專利、主要發現或其他有關價值等，作一綜合評估。

1. 請就研究內容與原計畫相符程度、達成預期目標情況作一綜合評估

■達成目標

□未達成目標（請說明，以 100 字為限）

□實驗失敗

□因故實驗中斷

□其他原因

說明：

2. 研究成果在學術期刊發表或申請專利等情形：

論文：■已發表 □未發表之文稿 □撰寫中 □無

專利：□已獲得 □申請中 ■無

技轉：□已技轉 □洽談中 ■無

其他：（以 100 字為限）

3. 請依學術成就、技術創新、社會影響等方面，評估研究成果之學術或應用價值（簡要敘述成果所代表之意義、價值、影響或進一步發展之可能性）（以 500 字為限）

在 2011 年，Kinjo 及其同事使用碳烯基(carbene)來穩定亞硼基(borylene)，近年來，含硼化合物被用來當作抗菌劑(antimicrobial agents) 、蛋白酶抑製劑(protease inhibitors)以及在硼中子俘獲治療(boron neutron capture therapy)中當成抗癌藥物(anticancer agents)的一部分。亞硼基可以扮演一個親核劑的角色，與其它缺電子化合物反應而形成一些含硼化合物，所以了解亞硼基的電子性質及反應性，是有其重要性的。因此我們已經利用了計算化學方法對其電子性質做了一詳盡的探討。不過，我們還沒有對其反應性進行探討，因而接下來我們打算探討其反應性。